

Citation for published version:

Latif, E, Ciupala, MA & Wijeyesekera, DC 2014, 'The comparative in situ hygrothermal performance of Hemp and Stone Wool insulations in vapour open timber frame wall panels', *Construction and Building Materials*, vol. 73, pp. 205-213. <https://doi.org/10.1016/j.conbuildmat.2014.09.060>

DOI:

[10.1016/j.conbuildmat.2014.09.060](https://doi.org/10.1016/j.conbuildmat.2014.09.060)

Publication date:

2014

Document Version

Peer reviewed version

[Link to publication](#)

Publisher Rights

CC BY-NC-ND

Published version available via: <http://dx.doi.org/10.1016/j.conbuildmat.2014.09.060>

University of Bath

Alternative formats

If you require this document in an alternative format, please contact:
openaccess@bath.ac.uk

General rights

Copyright and moral rights for the publications made accessible in the public portal are retained by the authors and/or other copyright owners and it is a condition of accessing publications that users recognise and abide by the legal requirements associated with these rights.

Take down policy

If you believe that this document breaches copyright please contact us providing details, and we will remove access to the work immediately and investigate your claim.

The comparative in situ hygrothermal performance of Hemp and Stone Wool insulations in vapour open timber frame wall panels

Eshrar Latif ^{a*}, Mihaela Anca Ciupala ^b, D C Wijeyesekera ^c

^a University of Bath, Bath, UK, ^b University of East London, London, UK, ^c University Tun Hussein Onn Malaysia, Johor, Malaysia

Abstract

An in situ experiment in a full scale timber frame test building was carried out to compare the hygrothermal performance of Hemp and Stone Wool insulations of identical thermal conductivity. Hemp and Stone Wool insulations were installed in timber frame wall panels without vapour barrier. The comparison was made in terms of heat transfer properties, likelihood of mould growth and condensation. Step changes in internal relative humidity were performed to explore the effect of high and normal internal moisture load on the wall panels. No significant difference between the average equivalent thermal transmittance (U-values) of the panels incorporating Hemp and Stone Wool insulations was observed. The average equivalent U-values of the panels were closer to the calculated U-values of the panels based on the manufacturers' declared thermal conductivity of Hemp and Stone Wool insulations. It was observed that the placement of heat flux sensor along the depth of the insulation had significant influence on the measured equivalent U-value of the panels during high internal moisture load. The frequency and likelihood of condensation was higher in the interface of Stone Wool and Oriented Strand Board (OSB). In terms of the parametric assessment of mould germination potential, relative humidity, temperature and exposure conditions in the insulation-OSB interfaces were found to be favourable to germination of mould spore. However, when the insulations were dismantled, no mould was visually detected.

Key words: Sustainable material, Hemp insulation, Stone Wool insulation, U -value, mould spore germination, condensation.

1. Introduction

About 45% of the total carbon emissions in the UK is caused by the domestic and non-domestic buildings [1]. Since the highest amount of energy is used for space heating [1], improved thermal insulation standard remains one of the most cost

* Corresponding author. Tel.: +44 7540606063. E-mail address: e.latif@bath.ac.uk (E. Latif).

effective means of reducing energy use [2] and thereby of reducing carbon emission. Most of the widely used thermal insulation materials are manufactured from either mineral or petro-chemical resources [3]. These resources are non-renewable and manufacturing processes of these insulation materials are energy intensive. In addition to reducing a building's operational energy use, there is also a conscious effort in the building industry to use natural, renewable and low-embodied energy building materials. Another trend in the building industry is to assess the applicability of walls that are hygroscopically active and do not require vapour barriers.

Hemp insulations are plant-based fibrous insulation materials. Limited amount of data is available on the hygrothermal performance of the Hemp insulations in a vapour open wall construction compared to that of any conventional insulation material. This paper aims to address this specific gap in knowledge. The comparisons between Hemp and Stone insulations are made in terms of equivalent thermal transmittance (U-value), likelihood of mould growth and condensation.

Research works on hygrothermal properties and performance of Hemp insulations are mostly based on experimental works in laboratories. Latif et al [4] determined the hygric properties of five Hemp insulations and Collet et al [5] assessed the moisture adsorption and vapour transfer properties of two types of fibrous Hemp-Wool insulations. These data can be used as input in hygrothermal software to numerically simulate the hygrothermal performance of the building envelopes incorporating these insulation materials. Korjenic et al [6] determined the moisture dependent thermal conductivity of Hemp insulation in steady state method by conditioning the insulations at a range of relative humidity conditions and then wrapping the insulations in foils before testing. However, in a vapour open construction during service conditions, moisture distribution in the insulation can be different from that

observed by wrapping insulations with impermeable membrane during laboratory tests. In terms of in situ performance monitoring, Nicolajsen [7] compared thermal transmittance of cellulose loose-fill insulation and Stone Wool insulation installed in a north facing timber frame wall in Denmark. In that test, the interior temperature and relative humidity were maintained at around 20°C and 60%, respectively. Stone Wool insulation was tested in a wall panel with vapour retarder and cellulose insulation was tested in wall panels with and without vapour retarder. The thermal transmittance value of the panels with 285 mm cellulose insulation for both panels was 0.14 W/m²K and the thermal transmittance value of Stone Wool was 0.12 W/m²K. For both applications of cellulose insulations, the maximum moisture content was 18% which is regarded as being within the safe range.

While Nicolajsen's study focusing on the exposure to 60% interior relative humidity is useful, it is also important to include the effect of changes in internal relative humidity on heat flux and interstitial relative humidity of wall panels in full scale tests. There are spaces in a house such as the kitchen and bathroom that are subject to sudden fluctuation of relative humidity. It is useful therefore to assess the effect of different ranges of internal relative humidity on average heat flux through thermal envelopes and on the likelihood of increased moisture content and mould growth in the thermal envelopes.

In terms of mould growth in Hemp insulations, Nykter [8] found that bast fibres of the Hemp insulations contained microbes from the very beginning of the fibre processing and, since the fibres contained nutrient, it was not possible to completely eliminate microbes.

There is not adequate information available on any full scale test in relation to the study of the in situ hygrothermal performance and parametric assessment of mould

growth in the Hemp insulation. The present paper attempted to address this gap in knowledge by assessing the in situ hygrothermal performance of Hemp and Stone Wool insulations in a full scale timber frame test building. The experimental test compared the hygrothermal performance of Hemp and Stone Wool insulations in vapour open wall panels in the internal boundary conditions incorporating very high (90%) and moderate interior relative humidity (50% to 60%). Additionally, the in situ test assessed the effect of the critical positioning of heat flux sensors along the depth of the wall panels on the equivalent U-values of the panels.

2. Theory

This section briefly describes the theories of determining thermal transmittance and assessing the likelihood of mould spore germination.

2.1 Thermal Properties

2.1.1 Method for numerical determination of U-value:

The calculations of U-value of the wall panels are based on BS EN ISO 6946:2007 [9]. The method is detailed below:

2.1.1.1 Calculation of the U-value of the panels consisting of homogeneous layers:

The total thermal resistance, R_T , of a plane building component consisting of thermally homogeneous layers perpendicular to the heat flow is given by the following expression:

$$R_T = R_{si} + R_1 + R_2 + \dots + R_n + R_{se} \quad [1]$$

Where

R_{si} is the internal surface thermal resistance

$R_1, R_2 \dots R_n$ are the design thermal resistance of each layer

R_{se} is the external surface thermal resistance

2.1.1.2 Calculation of the U-value of the panels consisting of homogeneous and inhomogeneous layers:

The total thermal resistance, R_T , of a building component consisting of homogeneous and inhomogeneous layers parallel to the surface is calculated as the arithmetic mean of the upper and lower limits of the resistance:

$$R_T = (R'_T + R''_T)/2 \quad [2]$$

Where

R'_T is the upper limit of total thermal resistance and R''_T is the lower limit of total thermal resistance. The upper limit of resistance, R'_T , is determined by assuming one-dimensional heat flow perpendicular to the surface of the component. It is given by the following expression:

$$1/R'_T = f_a/R_{Ta} + f_b/R_{Tb} + \dots + f_q/R_{Tq} \quad [3]$$

Where

$R_{Ta}, R_{Tb} \dots R_{Tq}$ are the thermal resistances from environment to environment for each section, calculated using equation [1]

$f_a, f_b \dots f_q$ are the fractional areas of each section.

Figure 1 shows the horizontal cross-section of a notional wall panel, where a, b and c are the width of each perpendicular section, d1, d2 and d3 are the thickness of layer 1, layer 2 and layer 3, respectively.

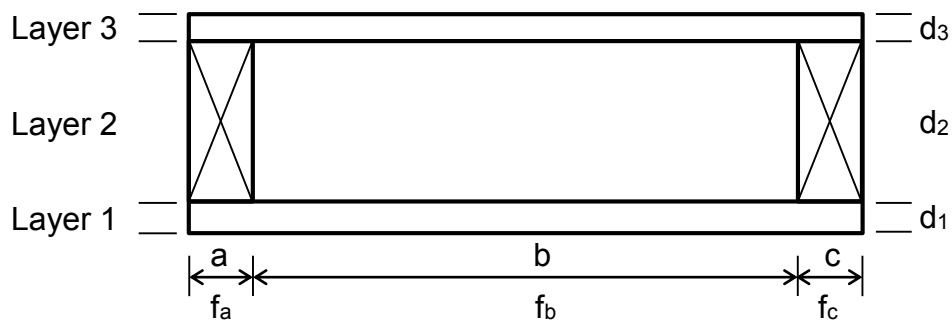


Fig.1. Horizontal cross-section of a notional wall panel.

The lower limit of total thermal resistance, R''_T , is determined by assuming that all planes parallel to the surfaces of the components are isothermal surfaces. The equivalent thermal resistance, R_j , for each thermally inhomogeneous layer is calculated using the following equation:

$$1/R_j = f_a/R_{aj} + f_b/R_{bj} + \dots + f_q/R_{qj} \quad [4]$$

Where

$R_{aj}, R_{bj}, \dots, R_{qj}$ are the thermal resistance of fractional areas f_a, f_b, \dots, f_q of layer j .

The lower limit of thermal conductivity is determined by using equation [1],

$$R''_T = R_{si} + R_1 + R_2 + \dots + R_n + R_{se} \quad [5]$$

2.1.1.3 Estimation of Error

The maximum relative error in thermal transmission, e , calculated as a percentage, is:

$$e = ((R'_T - R''_T) * 100) / (2 R_T) \quad [6]$$

2.1.2 In situ determination of U-value

ISO 9869 [10] describes the method for in-situ measurement of U-value of the building elements. U-value is obtained by dividing the mean density of heat flow rate by the mean internal and external temperature difference if the average U-value is taken over a long period of time, i.e. more than 72 hours' data for a heavy weight structure and at least three nights' data for a lightweight structure. The U-value is determined from the following equation:

$$U = \frac{\sum_{j=1}^n q_j}{\sum_{j=1}^n (T_{ij} - T_{ej})} \quad [7]$$

Where

U is thermal transmittance ($\text{W}/\text{m}^2\text{K}$), q is density of heat flow rate (W/m^2), T_i is interior ambient temperature ($^{\circ}\text{C}$), and T_e is exterior ambient temperature ($^{\circ}\text{C}$). In this paper the term ‘equivalent U-value’ is used instead of ‘U-value’ in relation to the in situ measurements to account for the added effect of relative humidity, enthalpy flow and phase change on heat flux through the building envelope.

2.2 Mould spore germination

The likelihood of germination and growth of mould on a surface depends on the combination of temperature, moisture, substrate type, exposure time and the type of species [11]. The relationship between these parameters in relation to the risk of mould spore germination is often expressed by isopleth curves [12]. Fig. 2 shows the germination isopleths, developed by Sedlbauer, incorporating the lowest isopleth for mould for substrate class 1 or biodegradable substrates (LIM I). The lowest isopleth for mould (LIM) curves are developed by analysing the combined growth conditions of all fungal species and thus this represents the worst-case scenario for mould spore germination.

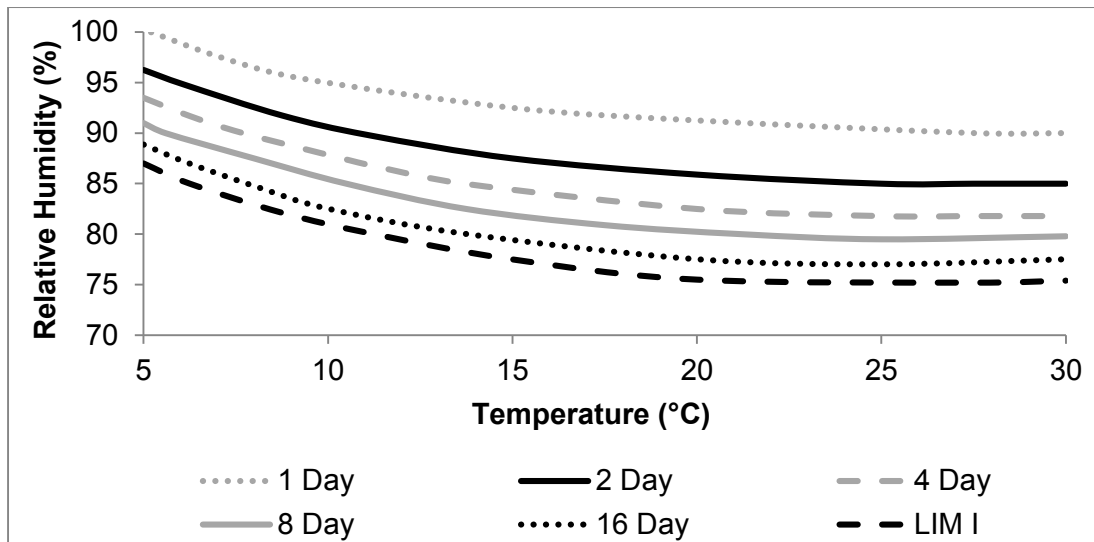


Fig. 2. Sedlbauer's isopleth system for substrate class I [12].

3. Material and method

3.1 The test materials

Hemp and Stone Wool insulation materials, with identical thermal conductivity, were sourced from the UK market. The key physical and thermal properties of the selected insulations are summarised in Table 1.

Table 1. Summary of the properties of the insulations.

Material	Density (Kg/m ³)	Thickness (mm)	Specific Heat Capacity (J/Kg°C)	Constituents	Manufacturers' Declared Thermal Conductivity (W/mK)
Hemp	50	100 (50 X 2)	1600	85% Hemp fibres, 10-12% bi-component fibres and 3-5% soda	0.038
Stone Wool	23	100	850	Amphibolite, about 6% lime Stone, about 9% calcium oxide, resin	0.038

Before installation, both Hemp and Stone Wool insulation materials were conditioned at $23 (\pm 2)^{\circ}\text{C}$ temperature and 50% relative humidity to simulate the level of hygrothermal exposure assumed to be encountered by insulations in manned storage spaces for construction materials. The adsorbed water contents in Hemp and Stone Wool for this exposure are 4.3 Kg/m^3 and 0.5 Kg/m^3 , respectively, determined from the values provided by Latif et al [4].

3.2 The test panels and sensors

3.2.1 The test panels

Two test panels (Fig. 3), Panel A with Stone Wool and Panel B with Hemp insulations, were incorporated in the eastern wall of a full scale timber frame test building. The 600 mm X 1800 mm test wall panels consist of a number of layers. From inside to outside, these layers are: 12.5 mm gypsum plasterboard (PB), 100 mm insulation, 11 mm OSB, 0.5 mm breather membrane, 25 mm air layer, 10 mm X 100 mm timber rain screen with 30 mm overlaps. Both panels are without a vapour barrier. Panel A and B are hygrothermally separated by a 50 mm wide section of expanded polystyrene (EPS) insulation.

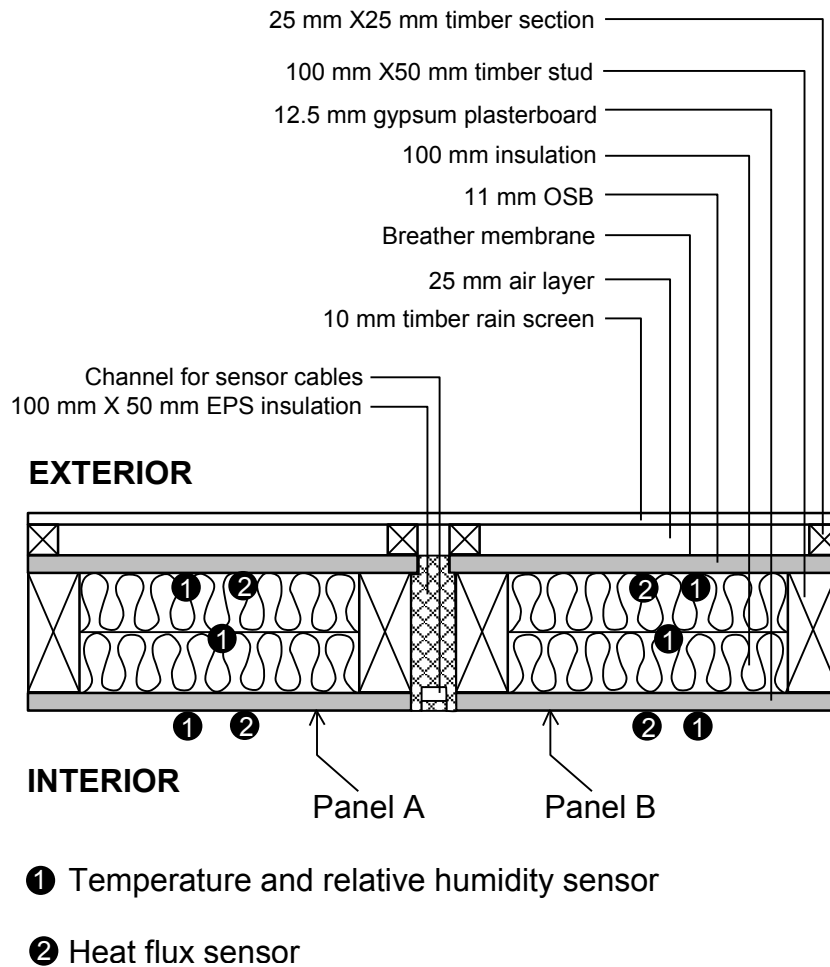


Fig. 3. Horizontal cross section of Panel A and Panel B with the sensors' location.

3.2.2 Sensors

Temperature and relative humidity sensors

CS215 temperature and relative humidity sensors from Campbell Scientific have been used to measure temperature and relative humidity together. The accuracy of the relative humidity measurement is (at 25 °C) $\pm 4\%$ over 0%-100% relative humidity while the accuracy of temperature measurement is ± 0.9 °C over -40 °C to +70 °C. The length of the sensor is 180 mm and average diameter is 15 mm.

Heat flux sensors

HFP01 heat flux sensors by Hukseflux, have been used to measure heat flux through the insulation. The measurement range is between -2000 W/m² and +2000 W/m² and the accuracy is $\pm 5\%$ on walls. The thickness of the sensor is 5 mm and the diameter is 80 mm. As the diameter of the heat flux sensor is smaller compared

to the dimension of the wall panels, the overall effect of the placement of the heat flux sensor on moisture flow can be assumed to be negligible.

3.3 The test building

The timber frame test building (Fig.4) was constructed near the Centre for Alternative Technology in Wales, UK. The timber frame test building was 3 metres long and 2.4 metres wide (Fig. 5). The height of the test building was 2 metres along the eaves and 2.4 metres along the ridge. The test building incorporated the two test wall panels in the eastern wall to accommodate the insulation samples. Except for the test wall panels, all the other walls, floor and roof of the test building were insulated with 100 mm expanded polystyrene (EPS) insulation (Fig.6) providing an approximate wall U-value of $0.3 \text{ W/m}^2\text{K}$.

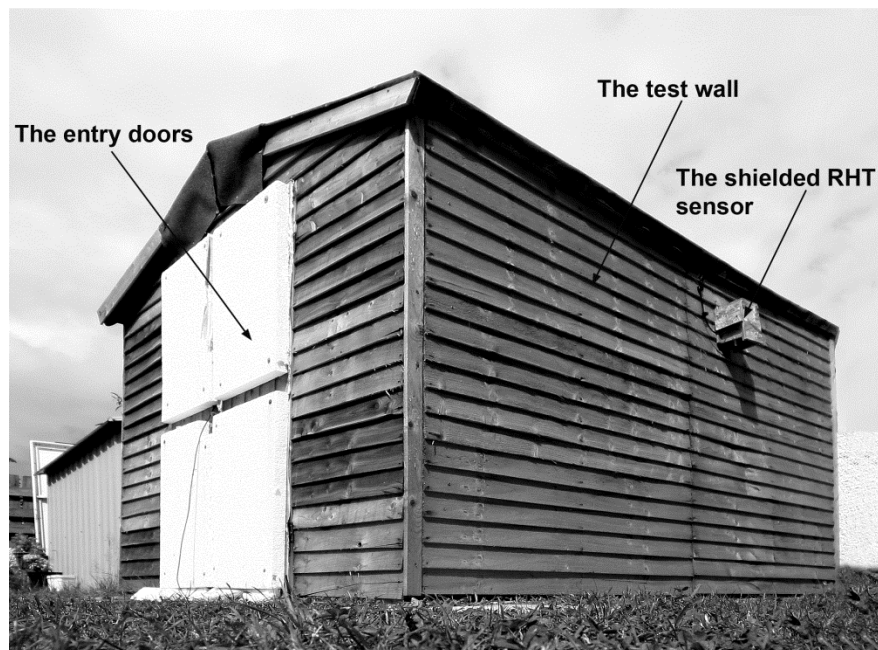


Fig. 4. The test building showing the position of the test wall, the entry doors and the temperature and relative humidity (RHT) sensor.

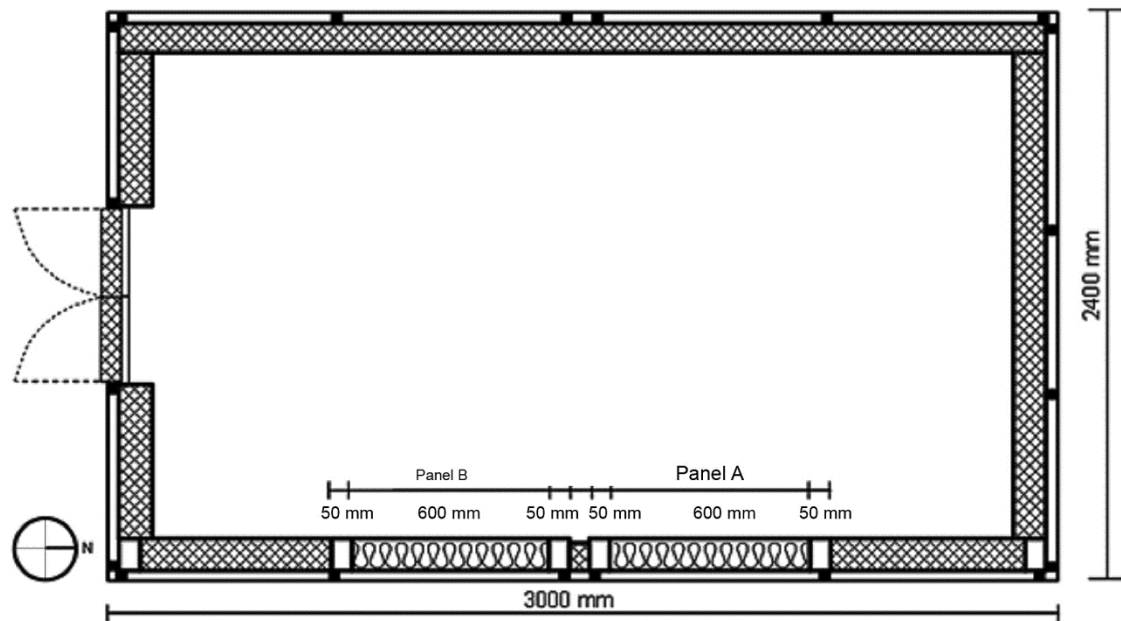


Fig. 5. Plan of the test building.

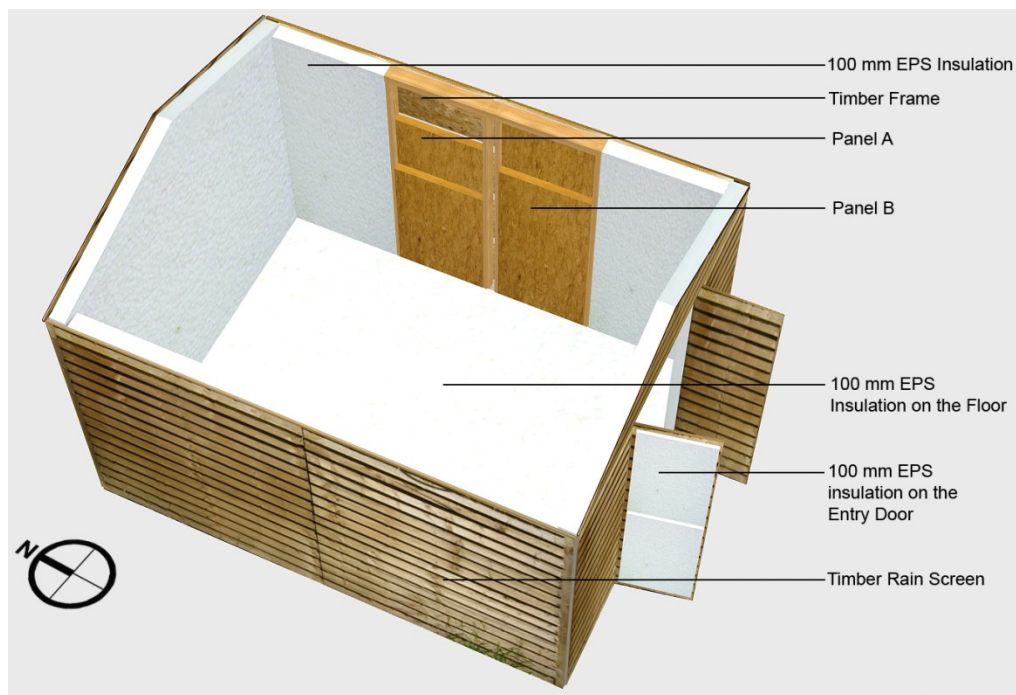


Fig. 6. 3-D computer image of the test building with the position of the test panels.

The east façade of the test building was completely shaded by other nearby buildings during the winter and 95% of the daytime during the summer. During the remaining 5% of the daytime during the summer, the solar radiation was only

incident on the 5% area of the eastern wall incorporating EPS insulation. For this reason, the heat flux through the eastern wall was not affected by the incident solar radiation. Hence, the eastern wall was suitable for assessing the thermal transmittance or U-value of the wall. The tests were conducted during July and August 2012. The averages of the maximum temperature, minimum temperature and mean temperature in the UK and Wales between 1910 and 2011 for the test months (Met Office, 2012) are shown in Table 2. The mean temperature condition in Wales is not significantly different from the mean temperature condition in the UK and thus can be considered as representative of the UK climate. Although rainfall in Wales and Scotland is the highest in the UK, this was not relevant for the tests as rain screen was used.

Table 2. Average external temperatures (temp) in the UK and Wales during July and August between 1920 and 2011.

	Maximum temp in the UK (°C)	Maximum temp in Wales (°C)	Mean temp in the UK (°C)	Mean temp in Wales (°C)	Minimum temp in the UK (°C)	Minimum temp in Wales (°C)
July	18.6	18.4	14.4	14.5	10.3	10.6
August	18.5	18.4	14.4	14.5	10.3	10.7

3.4 Instrumentation of the test building and the test panels

The relative humidity and temperature in the test building were set at the required test level by a shielded convective heater with thermostat and an evaporative industrial humidifier with hygostat.

The temperature and relative humidity sensors were installed at the following positions in Panel A and Panel B, as shown in Fig.3: one sensor at the insulation-

OSB interface, one at the middle of the insulation, one on the outer surface of the PB inner lining. One heat flux sensor was installed on the centre of the outer surface of the PB inner lining of each of the panel. The other heat flux sensor was placed in the centre of the insulation-OSB interface, which is between the outer surface of the insulation and the inner surface of the OSB board. In terms of placement of heat flux sensors, an assumption was made that if a heat flux sensor was installed on the insulation-OSB interface, it would register the added heat flux caused by phase change and enthalpy flow during high internal relativity, which might not be registered by the heat flux sensor installed on the inner surface. Thus, there would be a variation in the measured value of the equivalent U-value of panel A and B based on the heat flux data. Fig. 7 shows the vertical cross-section of the wall panels and the potential heat flux through the wall panels. Fig. 8 shows the finished setup of the instrumented test panels.

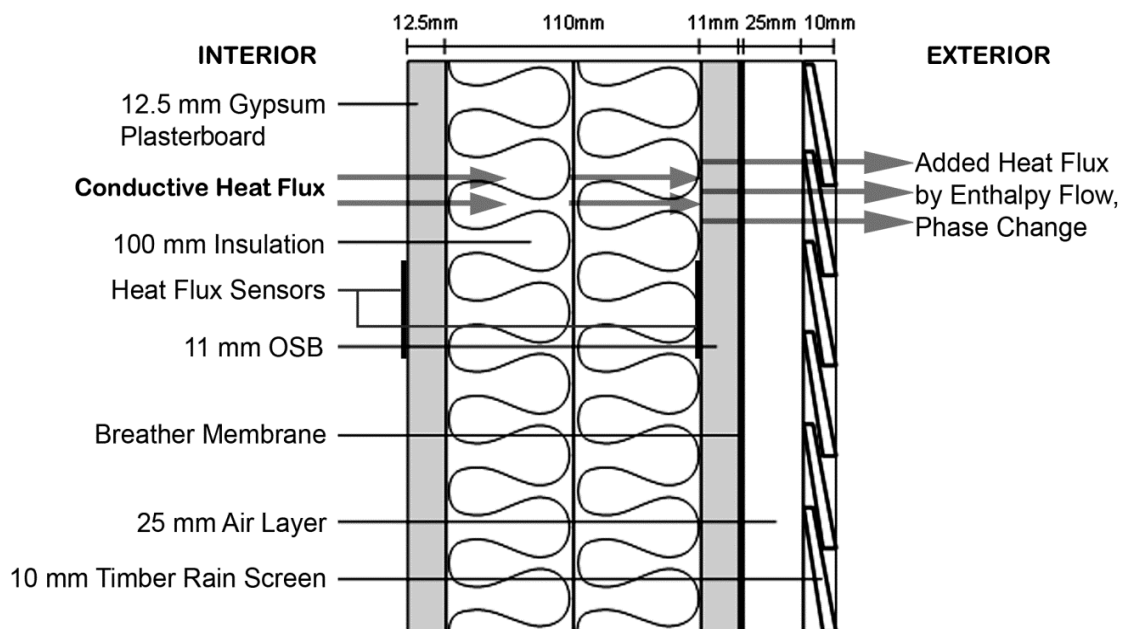


Fig. 7. Vertical cross section of the test wall panel.

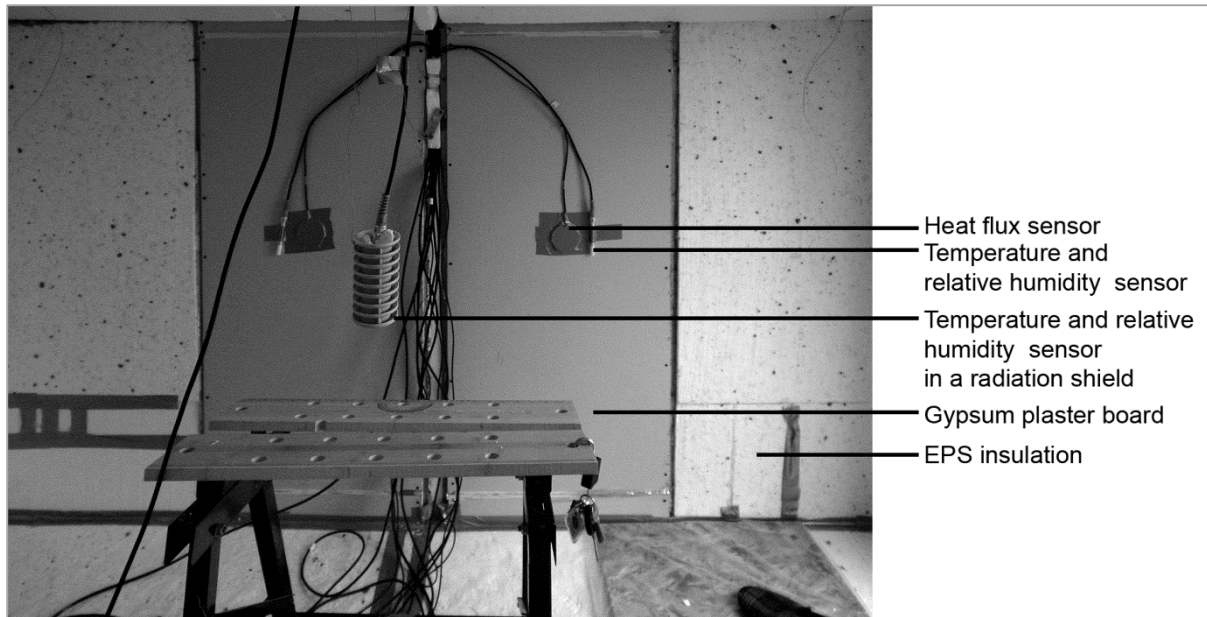


Fig. 8. The installed panels with the plasterboards and the sensors.

3.5 Operational errors in heat flux measurement

The ISO 9869 outlines the following likely operational errors in in-situ heat flux measurements 9869 [10]:

- a. The error due to the calibration of the heat flux sensor and the temperature sensors is about 5%.
- b. Random variation caused by difference in thermal contact between the sensors and the surface they are applied on. The corresponding error is about 5%.
- c. Operational error due to the modification of isotherms by the placement of heat flux sensors may vary between 2% to 3%. For the present test, the error is assumed as 2%.
- d. Errors due to the variations in temperature and heat flux over time. The error can be as much as 10% but can be reduced by taking data for a long period of time, keeping the variations in internal temperature low, etc.

- e. In addition to the errors in heat flux measurement, another 5% error is introduced to U-value measurement due to the temperature variations within the space and the difference between air and radiant temperature.

In terms of the error mentioned in (d), since the test wall was not in direct contact with sunlight and the internal variations of temperature were low, it can be assumed that the error was about 5%.

Thus, the total error in the U-value is calculated as the square root of sums of squares of the individual errors considered:

$$\text{Total error in U-value} = \sqrt{5^2 + 5^2 + 2^2 + 5^2 + 5^2} = 10.2\%$$

3.6 Experimental protocol

The in situ test was carried out in a timber frame test building, as described in subsection 3.3. Interior air velocity due to infiltration through the doors and convective air movement was 0.2 m/s. Table 3 shows the test set up and the duration of the test.

Table 3. The test setup and duration.

Wall Panel A	Wall Panel B	Inner lining in the panels	Interior air velocity (m/s)	Dates of test	Test duration
Stone Wool	Hemp	Gypsum plasterboard (PB)	0.2	From 19.07.12 to 27.08.12	39 days

The eastern wall of the test building contained wall Panel A with Stone Wool and wall Panel B with Hemp, as described in subsection 3.2. Both panels are without a vapour barrier. The interior temperature in the test building was maintained at 25 ± 4

°C. The duration of the test was about 39 days. In the current test, an attempt was made to find out the effect of repeated exposure to high and medium interior relative humidity on the hygrothermal conditions of the insulations. There was a continuous 13 days' period of exposure to 60 (± 5) % interior relative humidity during the test to determine the impact of the common interior relative humidity conditions on the insulation materials. **The test protocol is shown in Table 4.** The exterior of the test building was exposed to the external weather conditions during July and August 2012. Temperature and relative humidity of the interior, exterior and the wall panels were logged at every minute during the testing period.

Relative Humidity ($\pm 5\%$)	From	To	Days
35%	19/07/2012 10:00	21/07/2012 10:00	2
60%	21/07/2012 10:00	22/07/2012 10:00	1
90%	22/07/2012 10:00	24/07/2012 10:00	2
60%	24/07/2012 10:00	25/07/2012 10:00	1
35%	25/07/2012 10:00	28/07/2012 10:00	3
60%	28/07/2012 10:00	10/08/2012 10:00	13
85%	10/08/2012 10:00	11/08/2012 10:00	1
55%	11/08/2012 10:00	17/08/2012 10:00	6
90%	17/08/2012 10:00	18/08/2012 10:00	1
60%	18/08/2012 10:00	21/08/2012 10:00	3
90%	21/08/2012 10:00	23/08/2012 10:00	2
55%	23/08/2012 10:00	27/08/2012 10:00	4

3.7 Assessment of thermal performance and mould growth conditions

The U-values were calculated from the recorded experimental data using average method according to ISO 9869, as shown in equation 7. Mould growth condition was

assessed in terms of parametric studies. For parametric studies, the temperature-relative humidity relationships were plotted from the collected data and compared with the conditions for mould spore germination in Sedlbauer's isopleths.

4. Results and discussion

4.1 Temperature and Relative Humidity

Internal and external temperature and relative humidity conditions for 39-day testing period are shown in Fig. 9. Fig. 10 shows the resulting actual vapour pressure in the interior and exterior. It can be observed that the interior vapour pressure changed in response to the change in the interior relative humidity and compared to the interior vapour pressure, exterior vapour pressure remained steady.

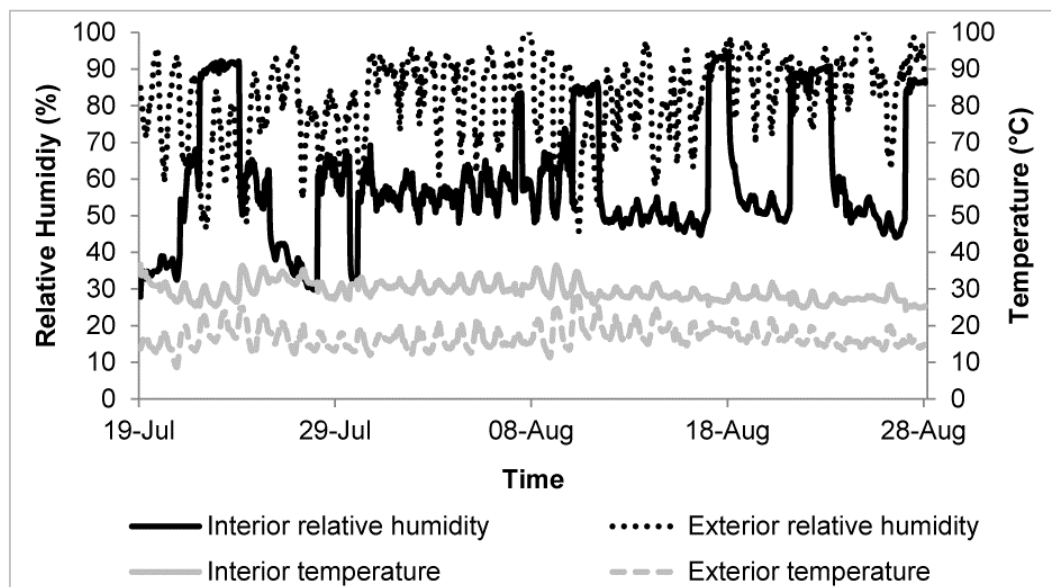


Fig. 9. The hygrothermal boundary conditions.

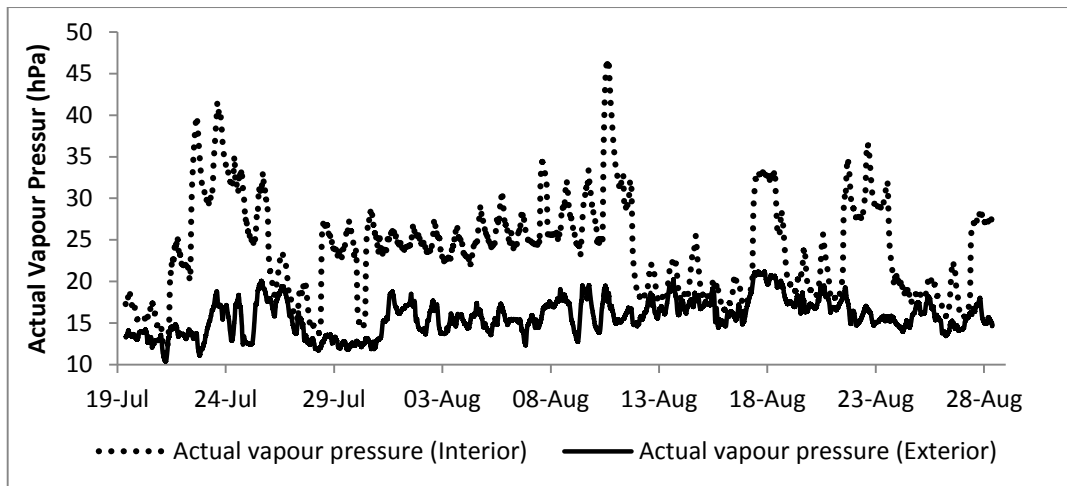


Fig. 10. Vapour pressure in interior and exterior.

4.2 Heat Flux and U-value

Fig. 11 and Fig. 12 show the heat flux and the differences between internal and external ambient temperature in the panels A and B. At high internal relative humidity, heat flux at the inner surface decreased (Fig.19) but increased at the insulation-OSB interface. As temperature difference did not increase during high relative humidity, the increase in heat flux in the insulation-OSB interface is plausibly due to enthalpy flow and phase change of moisture.

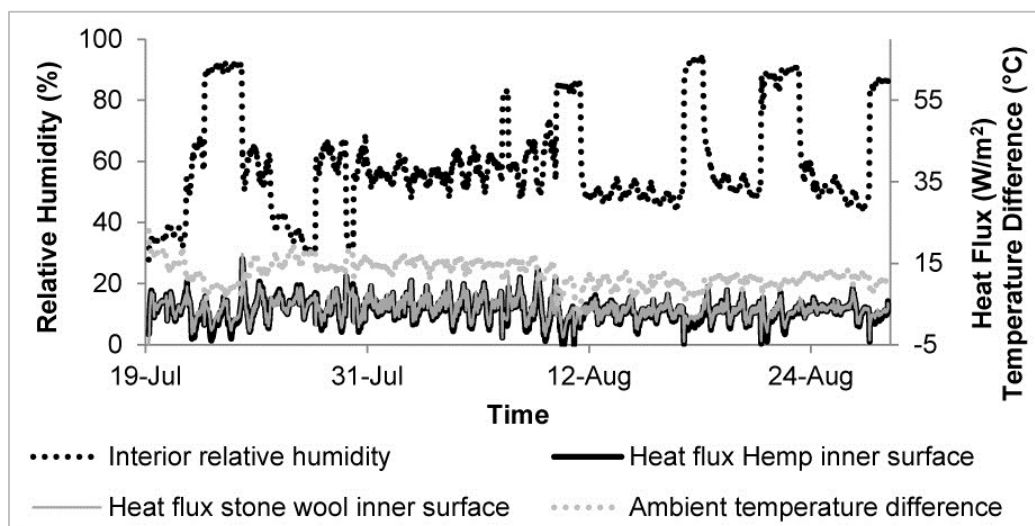


Fig. 11. Heat Flux in Panel A (Stone Wool) and Panel B (Hemp) based on the heat flux sensors located on the inner gypsum plasterboard surfaces.

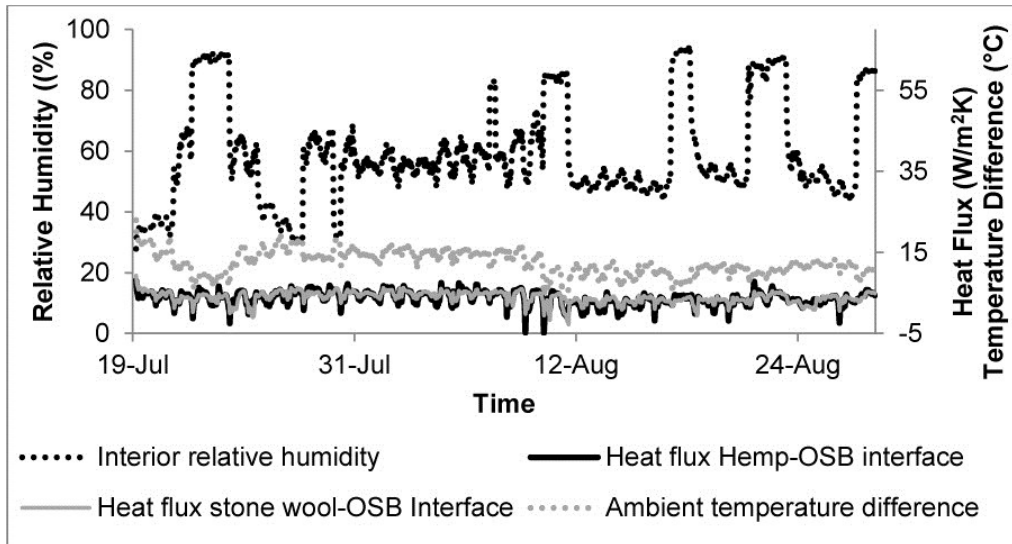


Fig. 12. Heat Flux in Panel A (Stone Wool) and Panel B (Hemp) based on the heat flux sensors located in the insulation-OSB interfaces.

The calculated U-value of the panels containing Stone Wool (Panel A) and Hemp (Panel B) insulations in dry condition, with and without considering the effect of thermal bridging through the timber studs, are shown in fig. 13.

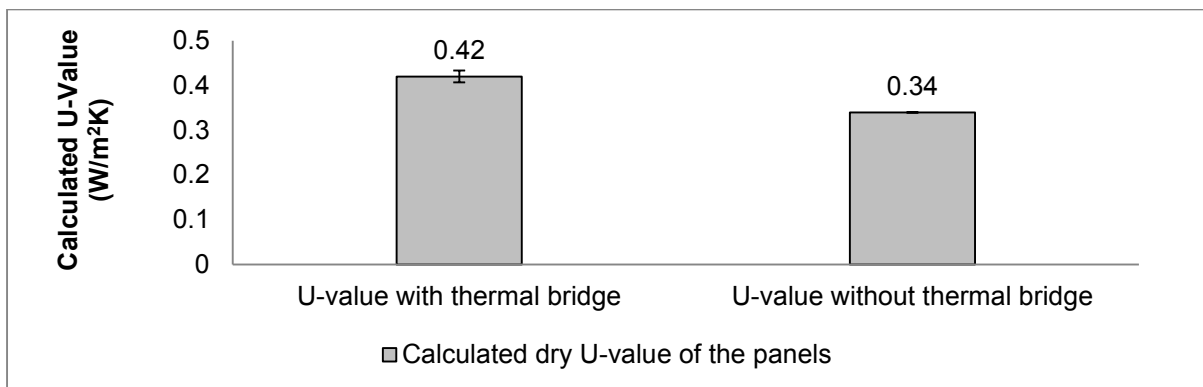


Fig. 13. Calculated U-values of wall panel A and B in dry condition with error bars.

Fig. 13 shows the in situ equivalent U-values of the insulation materials. In terms of the equivalent U-values of the panels obtained from the total period of the experiment at an average internal relative humidity of 59% and average temperature of 29.4°C, the equivalent U-value of Panel A derived from (Stone Wool)-OSB

interface ($0.30 \text{ W/m}^2\text{K}$) was lower than that derived from Stone Wool inner surface ($0.31 \text{ W/m}^2\text{K}$) by 3.3 %. The equivalent U-value of Panel B derived from the Hemp-OSB interface ($0.31 \text{ W/m}^2\text{K}$) was higher than that derived from Hemp inner surface ($0.28 \text{ W/m}^2\text{K}$) by 7.14 %.

In terms of equivalent U-values assessed during the average interior relative humidity of 56%, the equivalent U-value of Panel A derived from Stone Wool inner surface ($0.33 \text{ W/m}^2\text{K}$) was equal to that derived from (Stone Wool)-OSB interface. The equivalent U-value of Panel B derived from Hemp-OSB interface ($0.32 \text{ W/m}^2\text{K}$) was higher than that derived from Hemp-2 inner surface ($0.30 \text{ W/m}^2\text{K}$) by 6.67%.

In terms of equivalent U-values assessed during the average interior relative humidity of 90%, in line with the assumption made in subsection 4.2, the equivalent U-value derived from (Stone Wool)-OSB interface ($0.44 \text{ W/m}^2\text{K}$) was higher than that derived from Stone Wool inner surface ($0.27 \text{ W/m}^2\text{K}$) by 63% and the equivalent U-value derived from Hemp-OSB interface ($0.46 \text{ W/m}^2\text{K}$) was higher than that derived from Hemp inner surface ($0.17 \text{ W/m}^2\text{K}$) by 170%. It is plausible that the increased U-value in the insulation-OSB interfaces at high relative humidity is due to the effect of moisture movement and phase change.

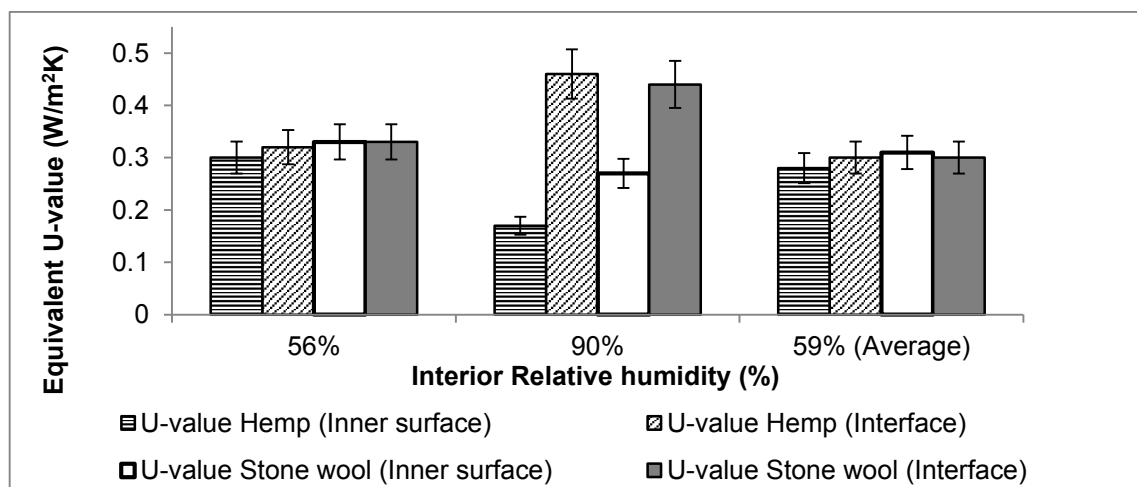


Fig. 14. The equivalent U-values of the insulations with error bars.

However, it can also be observed in Fig. 14 that the average in situ equivalent U-values of both panels are lower than the calculated U-values (Fig. 13) of the panels, with or without taking into account the effect of thermal bridge. The likely reasons for the lower average thermal conductivity values are: firstly, the internal relative humidity was equal to or less than 60% for 84.6% of the total period of experiment and secondly, the effect of the variable heat capacity of the insulation due to the dynamic hygrothermal boundary condition.

4.3 Relative humidity and prediction of mould spore germination

Fig. 15 shows the relative humidity conditions in the insulation-OSB interfaces in wall Panel A (Stone Wool) and Panel B (Hemp) along with the interior relative humidity for the total duration of the test. The average temperature in the interfaces of stone wool and hemp insulation was 20.7°C and 20.6°C, respectively.

Except for the period between 27 and 28 July 2012, the relative humidity values in the insulation-OSB interfaces were always more than 80%. The key difference between Hemp and Stone Wool insulation in terms of hygric response was that the interface between Stone Wool and OSB frequently reached 100% relative humidity value which never occurred in the Hemp-OSB interface.

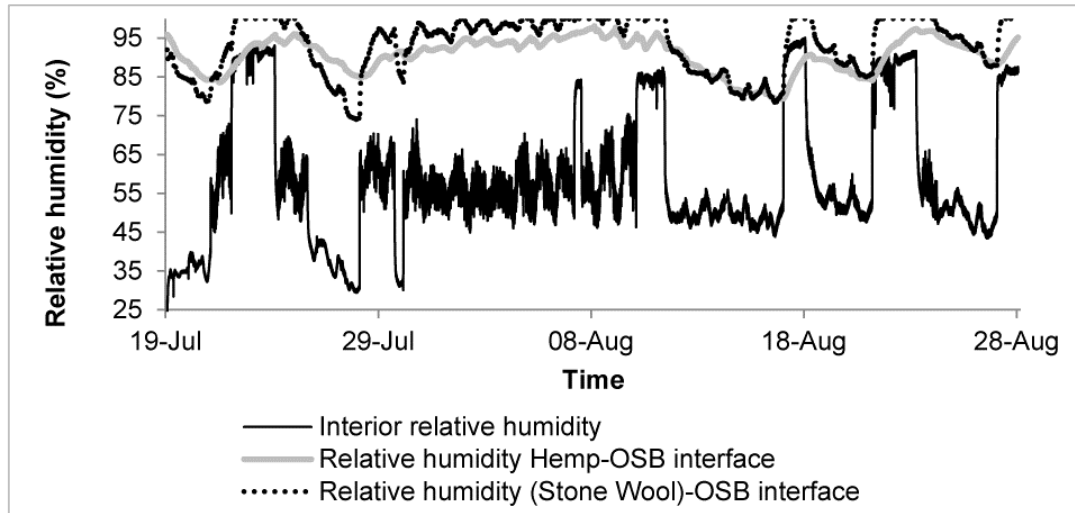


Fig. 15. The relative humidity conditions at insulation-OSB interfaces.

Fig. 16 shows the hygric conditions in the insulation-OSB interface of Hemp and Stone Wool insulation materials between 19 and 26 July 2012. It can be observed that when interior relative humidity increased from 60% to 90%, the relative humidity in (Stone Wool)-OSB interface immediately rose up to 100%, while the relative humidity in Hemp-OSB interface increased to about 78%. During the whole duration of the interior relative humidity of about 90%, the (Stone Wool)-OSB interface relative humidity always stayed at 100% while the Hemp-OSB interface relative humidity slowly increased to 95%. The slower increase in relative humidity in the Hemp-OSB interface is assumed to be due to the fact the moisture adsorption capacity is very high in hemp insulation and negligible in stone wool insulation as explained in Latif et al [4].

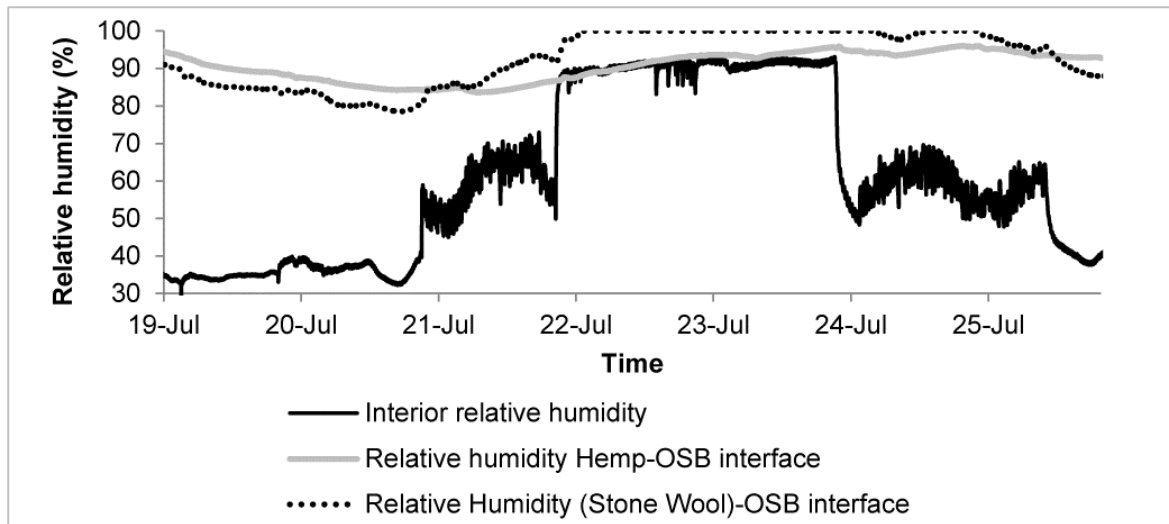


Fig. 16. The insulation-OSB interface hygric conditions for 7 days.

Fig. 17 presents the temperature and relative humidity conditions in the (Stone Wool)-OSB interface of Panel A in conjunction with the Sedlbauer's isotherms for substrate class I. The hygrothermal conditions in the (Stone Wool)-OSB interface in the Panel A during the 39-day long experiment were most of the time above the LIM I isopleth. Fig. 18 shows the graph of continuous 11 days when the hygrothermal conditions were well above the 1-day isopleth. The germination of mould spore was highly likely during those 11 days.

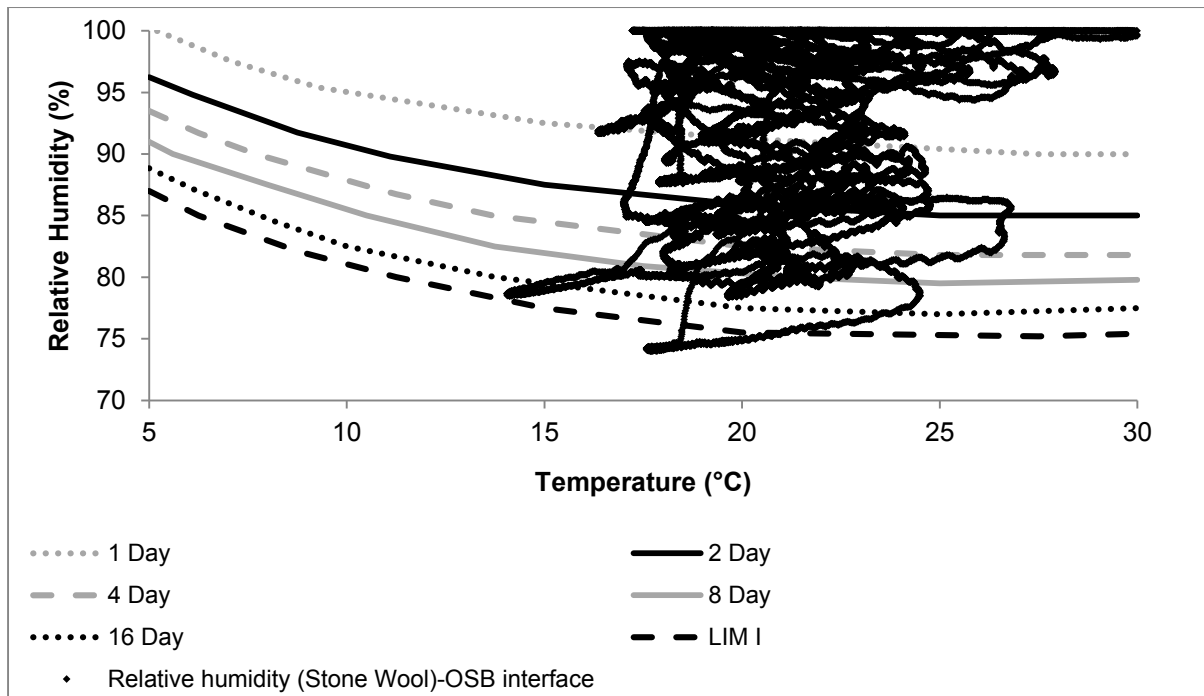


Fig. 17. 39 days' hygrothermal conditions in the (Stone Wool)-OSB Interface.

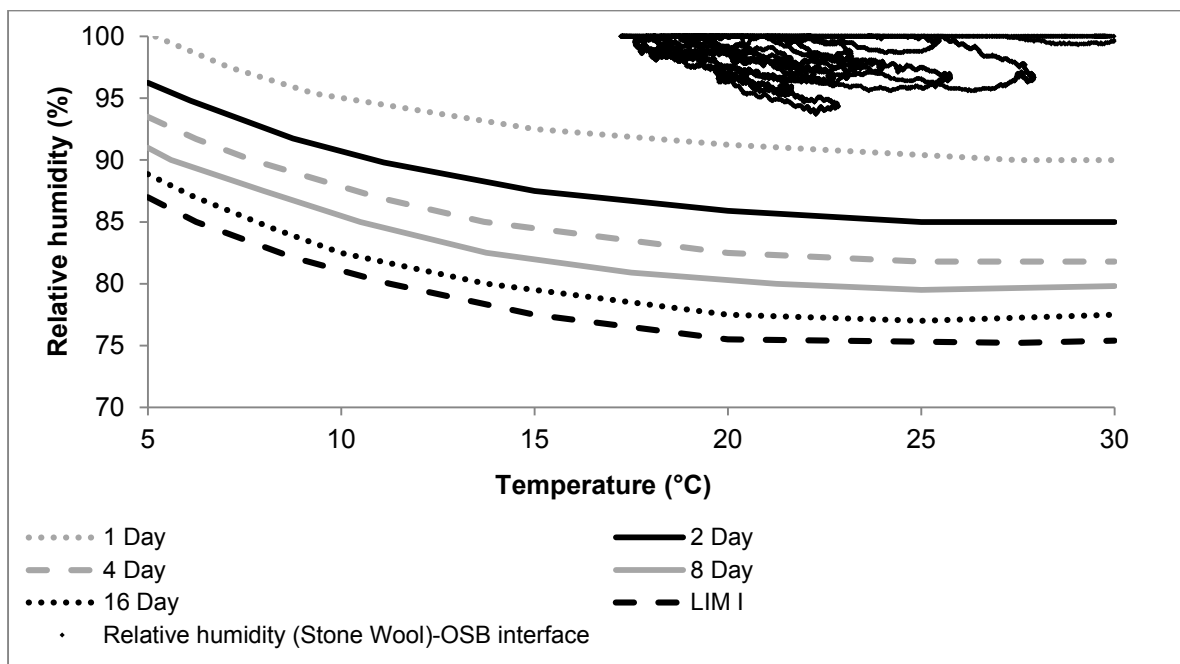


Fig. 18. Continuous 11 days' hygrothermal condition in (Stone Wool)-OSB interface.

Fig. 19 shows the temperature and relative humidity conditions in the Hemp-OSB interface of Panel B with reference to the Sedlbauer's isopleth for substrate class I. The hygrothermal conditions are above the 8-day isopleth most of the time. Fig. 20

shows continuous 11 days' hygrothermal conditions in the Hemp-OSB interface. The hygrothermal conditions are mostly above the 1-day isopleth, implying that germination of mould spore is highly likely during this period.

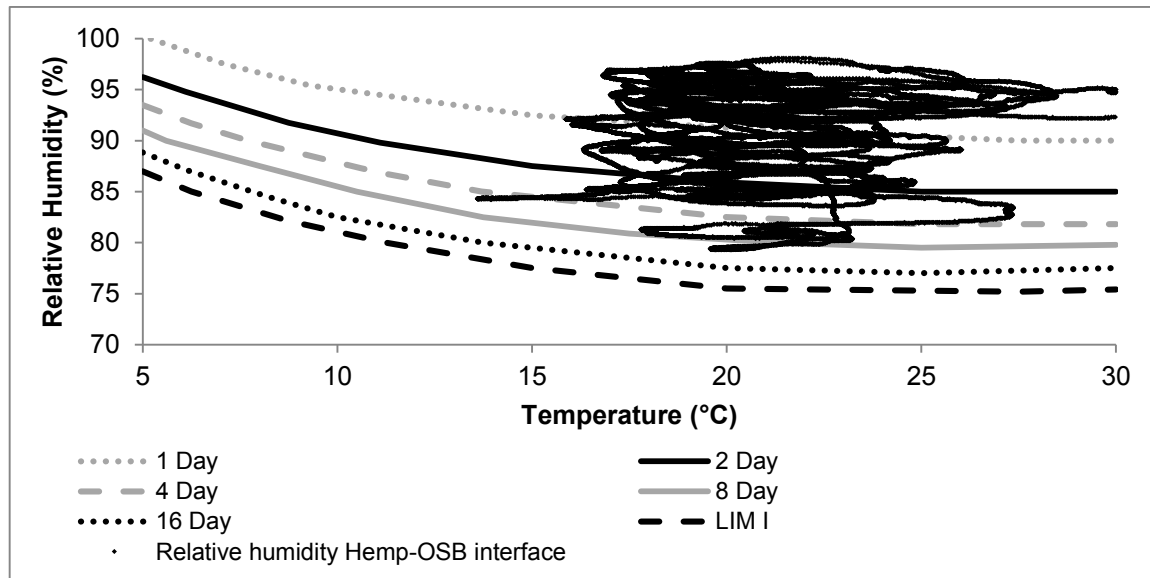


Fig. 19. 39 days' hygrothermal condition in Hemp-OSB Interface.

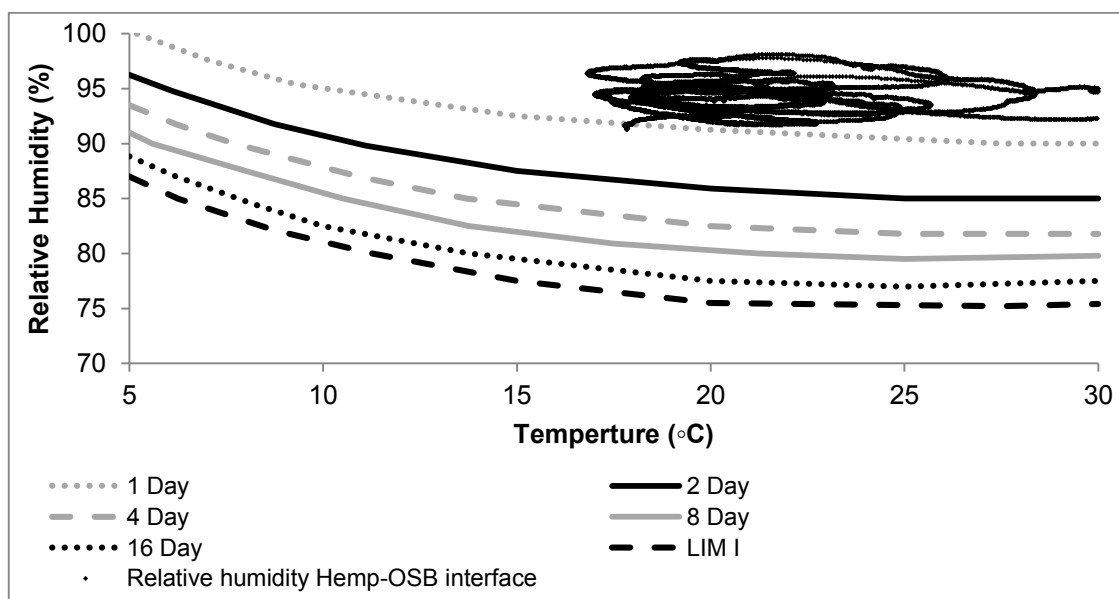


Fig. 20. Continuous 11 days' hygrothermal condition in Hemp-OSB interface.

Despite the predictions of mould spore germination, no visible evidence of mould growth was observed in the external faces of insulations when the insulations were dismantled. The possible reasons for this are: firstly, the insulations may have been

pre-treated with anti-fungal agent, secondly, the limiting time for mould spore germination in Sedlbauer's isopleth may need modification for dynamic hygrothermal boundary conditions.

When the insulation materials were dismantled at the end of the test, condensation was observed only on the impermeable surface of the temperature and relative humidity sensor in the (Stone Wool)-OSB interface. Therefore, it is plausible that some condensation occurred on the OSB surface of the (Stone Wool)-OSB interface and the condensates were readily absorbed by the OSB. No condensation or wet surface was observed in the Hemp-OSB interface.

5. Conclusion

The paper focused on the assessment and comparison of the in situ hygrothermal performance of Hemp and Stone Wool insulation materials of identical thermal conductivity in identical hygrothermal boundary conditions. In terms of equivalent U-value, no significant difference was observed between the panels incorporating Stone Wool (Panel A) and Hemp (Panel B) insulations. Both panels A and B showed equivalent U-values lower than the U-values of the panels derived from numerical calculation according to BS EN ISO 6946:2007. At 90% internal relative humidity, significant difference ranging from 63% to 170% was observed between the U-values of each panel depending on the type of insulation and placement of the heat flux sensors. With regards to Sedlbauer's isopleths of mould spore germination, while hygrothermal condition in the insulation-OSB interfaces of both Hemp and Stone Wool insulation materials seemed to favour mould spore germination, Stone Wool was more susceptible to this than Hemp. In terms of the risk of interstitial condensation, the relative humidity in the (Stone Wool)-OSB interface frequently

rose to 100%, implying that there was a likelihood of frequent condensation in the (Stone Wool)-OSB interface. Compared to Stone Wool, the frequency and likelihood of occurrence of condensation seemed to be lower in Hemp-OSB interface.

References

- [1] IGT. Low carbon construction : final report. London: Dept. of Business, Innovation and Skills; 2010.
- [2] Mackenzie F, Pout C, Shorrock L, Matthews A, Henderson J. Energy efficiency in new and existing buildings : comparative costs and CO2 savings. Bracknell: BRE Press; 2010.
- [3] Bevan R, Woolley T. Hemp lime construction : a guide to building with hemp lime composites. Bracknell: IHS BRE Press; 2008.
- [4] Latif E, Tucker S, Ciupala MA, Wiyjeyesekera DC, Newport D. Hygric Properties of Five Hemp Bio-Insulations with Different Compositions. *Construction and Building Materials*. 2014;66(C):702-711.
- [5] Collet F, Achchaq F, Djellab K, Marmoret BH. Water vapor properties of two hemp wools manufactured with different treatments. *Construction and Building Materials*. 2011;25:1079-85.
- [6] Korjenic A, Petráněk V, Zach J, Jitka H, J. Development and performance evaluation of natural thermal-insulation materials composed of renewable resources. *Energy and Buildings*. 2011;43:2518-23.
- [7] Nicolajsen A. Thermal transmittance of a cellulose loose-fill insulation material. *Building and Environment*. 2005;40:pp. 907-14.
- [8] Nykter M. Microbial quality of hemp (*cannabis sativa* L.) and flax (*linum usitatissimum* L.) from plants to thermal insulation'. Helsinki: University of Helsinki; 2006.
- [9] Institute BS. BS EN ISO 6946. Building components and building elements. Thermal resistance and thermal transmittance. Calculation method. 2007.
- [10] ISO 9869. Thermal insulation-Building elements -In-situ measurement of thermal resistance and thermal transmittance. Switzerland: International Organization for Standardization; 1994.
- [11] Viitanen H, Vinha J, Salminen K, Ojanen T, Peuhkuri R, Paajanen L, et al. Moisture and Bio-deterioration Risk of Building Materials and Structures. 2010;33(3):201-24.
- [12] Vereecken E, Roels S. Review of mould prediction models and their influence on mould risk evaluation. *Building and Environment*. 2012;51:296-310.